**ORIGINAL PAPER**

# Surrogate Models to Predict the Long-Term Compressive Strength of Cement-Based Mortar Modified with Fly Ash

Aso Abdalla[1] · Ahmed Salih Mohammed[1] 📵

## Abstract

In the recent decade, supplementary cementing ingredients have become an essential part of various strength ranges of concrete and cement-mortar mix design. Examples are natural materials, by-products, industrial wastes, and materials that require less energy and time to generate. Fly ash is one of the most widely utilized additional cementing ingredients. Fly ash is a by-product substance produced by coal combustion. It's being used in cement mortar and concrete as a pozzolanic substance. It has demonstrated significant influence in improving liquid and solid properties of cement mortar, such as compressive strength. Multi Expression Programming (MEP) is employed in this study to estimate the compressive strength (CS) of cement mortar modified with fly ash. The outcomes of this model were compared and evaluated with several other models such as the Nonlinear Regression model (NLR), Artificial Neural Network (ANN), and M5P-tree models that have been used in the construction fields. The input parameters included water/cement ratio (w/c), curing time (t days), and fly ash content (FA %), while the target property was compressive strength up to 360 days of curing. Four hundred fifty (450) data are collected from previous literature on modifying cement mortar with fly ash for that purpose. The water/cement ratio ranged from 0.24 to 1.2, and the fly ash was used to replace cement up to 55% (%wt. of dry cement). Based on the Coefficient of Determination ($R^2$), Root Mean Squared Error (RMSE), Scatter Index (SI), Objective (OBJ), Mean Absolute Error (MAE), t-test value, the uncertainty of 95%, Performance Index ($\rho$), and boxplot for actual and predicted compressive strength. The MEP model performed better than other developed models according to evaluation tools. The compressive strength was also correlated with flexural and splitting tensile strengths using different nonlinear models.

## 1 Introduction

Management of industrial waste materials is a global problem; fly ash (FA) is a waste-product of power plants resulting from coal combustion. Supplementary cementitious materials (SCM) are those materials that are used in concrete plants to replace Portland cement in cement-based mortar and cement-based concrete. The hydration of cement with water forming calcium silicate hydroxide gel (C–S–H) and calcium silicate (C–H), SCM like fly ash reacted with C–H and resulted in the formation of further C–S–H and solving the durability problems related to C–H which is vulnerable to chemical attack [1]. Fly ash modified cementitious

material generate less heat during the hydration process; therefore, it is suitable for mass concrete [2–6], and their strength is greatly influenced by the physical characteristics and chemical composition of the fly ash; those properties depend on the coal type and the equipment used in the power plant and the reactivity of the fly ash [6, 7]. The pozzolanic reactivity of fly ash has been investigated in various research. Pozzolanic reactivity of fly ash can be measured through chemical analysis to determine the quantity of silica or measuring the heat developed at the hydration time. However, since the silicate forms a gel at a pH greater than 10, the amount of silica used in the gel formation must be considered [8, 9]. After 28 days of curing, the consumption of C–H through a pozzolanic reaction of fly ash can be measured by X-Ray diffraction (XRD) or thermal analysis [10]. Natural hydraulic lime occurs from the calcination and subsequent slaking of marly limestones (limestones with clay impurities, which after calcination become reactive silicates and aluminates). It thus sets through both hydration and carbonation processes, leading to the formation of

✉ Aso Abdalla
aso.abdalla@univsul.edu.iq

✉ Ahmed Salih Mohammed
ahmed.mohammed@univsul.edu.iq

1 Civil Engineering Department, College of Engineering, University of Sulaimani, Kurdistan, Iraq

hydraulic compounds and the formation of calcite, respectively. Due to the relatively low calcination temperatures required, it is considered as an eco-friendly material in relation to modern binders, such as cement, as also pointed out by [11]; furthermore, during hardening, part of the $CO_2$ emitted through the limestone calcination is consumed during the carbonation process, thus further lowering the total environmental impact associated to the greenhouse effect gases [11]. Cho et al. [12] evaluated the effect of fly ash chemical composition on the compressive strength of fly ash modified cement mortar using sixteen different types of fly ashes for replacing cement in cement mortar. They concluded that the pozzolanic reactively of fly ash is mainly affected by the percentage of $SiO_2$, $Al_2O_3$, and $Fe_2O_3$, and the fly ash effect on compressive strength at 90 days of curing is greater than compressive strength at 28 days of curing. Chindaprasirt et al. [13] studied the effect of fly ash fineness on the mechanical properties, sulfate resistance, and drying shrinkage of cement mortar. The study results showed that fly ash with higher fineness improves strength, drying shrinkage, and sulfate attack. Chindaprasirt et al. [14] evaluated workability and chloride ion resistance of cement mortar modified with fly ash. Replacement of cement with fly ash improved resistance to Chloride ion penetration and better workability for the cement mortar.

Modeling the properties of materials can be performed in various ways, including computational modeling, statistical techniques, and newly created tools like Regression analysis, M5P-tree, and artificial neural networks (ANN) [15–19].

Mohammed et al. [20] used ANN, M5P tree, and nonlinear regression to predict the compressive strength of cement-based mortar modified with fly ash. They have concluded that the ANN model can be used efficiently with a high correlation coefficient (R) and minimum RMSE. ANN model was also used by Apostolopoulou et al. [11] to predict the compressive strength of natural hydraulic lime; the results revealed that ANN could accurately forecast the CS of natural hydraulic lime mortars, implying that they can be used as a decision-making tool when developing natural hydraulic lime mortars. Also, Armaghani and Asteris [21] investigated the application of ANN and adaptive neuro-fuzzy inference system (ANFIS) models to predict the compressive strength of cement mortar with or without metakaolin concluded that ANFIS performed better than ANN. At the same time, overfitting was observed for some of the data. Despite the extensive use of mortar materials in constructions over the last decades, there is not yet a reliable and robust method available in the literature to estimate its strength based on its mix parameters. This limitation is due to the highly nonlinear relation between the mortar's compressive strength and the mixed components. This paper investigates the application of artificial intelligence techniques to predict the compressive strength of cement-based mortar materials with or

without metakaolin. Specifically, surrogate models (such as artificial neural network, ANN and adaptive neuro-fuzzy inference system, ANFIS models) have been developed to predict the compressive strength of mortars trained using experimental data available in the literature. The comparison of the derived results with the experimental findings demonstrates the ability of both ANN and ANFIS models to approximate the compressive strength of mortars reliably and robustly. Although ANFIS obtained higher performance prediction to estimate the compressive strength of mortars compared to the ANN model, it was found through the verification process of some other additional data, the ANFIS model has overfitted the data. Therefore, the developed ANN model has been introduced as the best predictive technique for solving the problem of the compressive strength of mortars. Furthermore, an ambitious attempt to reveal the nature of mortar materials has been made [22, 23]. soft computing techniques in estimating concrete's compressive strength (CS) utilizing two non-destructive tests, namely ultrasonic pulse velocity and rebound hammer test. Specifically, six conventional soft computing models were used: back-propagation neural network (BPNN), relevance vector machine, minimax probability machine regression, genetic programming, Gaussian process regression, and multivariate adaptive regression spline. To construct and validate these models, 629 datasets were collected from the literature. Experimental results show that the BPNN attained the most accurate prediction of concrete CS based on both ultrasonic pulse velocity and rebound number values. The results of the employed MARS and BPNN models are significantly better than those obtained in earlier studies. Thus, these two models can assist engineers in the design phase of civil engineering projects to estimate the concrete CS with a greater accuracy level [23]. An experimental database consisting of 1030 records has been compiled from the machine learning repository of the University of California, Irvine. The database was used to train and validate four conventional machine learning (CML) models, namely Artificial Neural Network (ANN), Linear and Non-Linear Multivariate Adaptive Regression Splines (MARS-L and MARS-C), Gaussian Process Regression (GPR), and Minimax Probability Machine Regression (MPMR). Subsequently, the predicted outputs of CML models were combined and trained using ANN to construct the Hybrid Ensemble Model (HENSM). It is observed that the proposed HENSM produces higher predictive accuracy compared to the CML models used in the present study. The predictive performance of all models for CS prediction was compared using the testing dataset. The HENSM model attained the highest predictive accuracy in both phases. Based on the experimental results, the newly constructed HENSM model is very potential to be a new alternative in handling the overfitting issues of CML models and hence, can be used to predict the concrete CS, including

the design of less polluting and more sustainable concrete constructions [24]. Metakaolin is used as an additive in cement mortars, substituting the cement fraction to a certain extent, to enhance the sustainability of cement mortars, both in terms of the environmental impact of raw materials production and in terms of the environmental impact of raw materials production improving cement-based mortars durability under environmental actions. However, as metakaolin affects the mechanical performance of cement-based mortars, it is important to know the compressive strength that these blended mortars achieve at 28-days in terms of structural design. Toward this direction, metaheuristic models such as ANN and Genetic Programming (GP) models have been developed and trained through the use of a database, compiled by available, in the literature, experimental works related to cement and blended cement-metakaolin mortars. In the model development phase, the most important parameters affecting the strength of concrete-based mortars were investigated and selected. In addition, the effect of the selected transfer functions and the initial values of weights and biases on the performance of ANN models were also investigated. Based on this analysis, it was shown that ANNs with selected transfer functions (such as the Radial-Basis transfer function, the Soft-Max transfer function, and the Normalized Radial Basis transfer function) were able to reliably simulate the 28-days compressive strength of the cement-based mortars. In addition, it was shown that parameters such as the cement grade and the maximum diameter of aggregates are very important in determining the compressive strength of the cement-based mortars; this is an important finding, because these parameters are usually not taken into account in the research studies concerned in the prediction of compressive strength through computational models [25].

In this study, the MEP model was used to predict the compressive strength of the fly ash modified cement-mortar using 450 data collected from previous research related to modified cement-based mortar, and outcomes were compared with different approaches, including ANN, nonlinear regression, M5P-tree, and nonlinear model. The various statistical evaluations were applied to assess the accuracy of the models. The correlation between the compressive with flexural and splitting strengths of fly ash-modified cement-based mortar using different nonlinear models.

# 2 Objectives

This study is aimed to investigate the application of the MEP model to forecast the compressive strength of cement-based mortar with or without fly ash up to 360 days curing; the followings are the main objectives:

(i) Statistically analyze the collected data to evaluate the effect of the mix proportion of cement-based mortar modified with fly ash on the compressive strength.

(ii) Developing a reliable model to predict the compressive strength of cement mortar modified with fly ash and obtaining the sensitivity of the models using different statistical approaches.

(iii) Correlating compressive strength of the cement mortar with flexural and splitting tensile strengths of the cement mortar modified with fly ash.

# 3 Methodology

Figure 1 presents the steps that have been followed during this study. The following are steps of the current study methodology:

(i) Collecting a considerable number of the datasets (450 datasets) from different published studies in reputable journals.

(ii) Considering w/c, curing time, and fly ash content as independent variables for predictors and compressive strength of the cement-based mortar as a target.

(iii) Dividing the collected data into three datasets, 70% for training 30% for testing and validation.

(iv) Statistical analysis, visualizing data and determining the correlation between independent and dependent variables.

(v) Modeling the compressive strength using MEP, NLR, ANN, and M5P-tree models.

(vi) Evaluating developed models based on $R^2$, RMSE, SI, MAE, OBJ, t-test, 95% uncertainty, and performance index for actual and predicted compressive strength.

(vii) Performing sensitivity analysis to detect the most dominant parameter on the compressive strength of cement-based mortar modified with fly ash.

## 3.1 Data Collection

A comprehensive 450 data on compressive strength and flexural strength data on cement-based mortar modified with fly ash were collected from different literature [20, 24–38]. The dataset was divided into three groups (training, testing, and validating) randomly using the Rand function in Microsoft Excel. The largest group included 70% of the dataset (300 data), and each of the other two groups had 15% of the dataset (75 data). The training data is used to develop the model while validating and testing data is provided to test the developed model against unseen data. The overfitting of the developed model can be minimized [39]. The summary

**Fig. 1** Methodology flowchart
of the current study
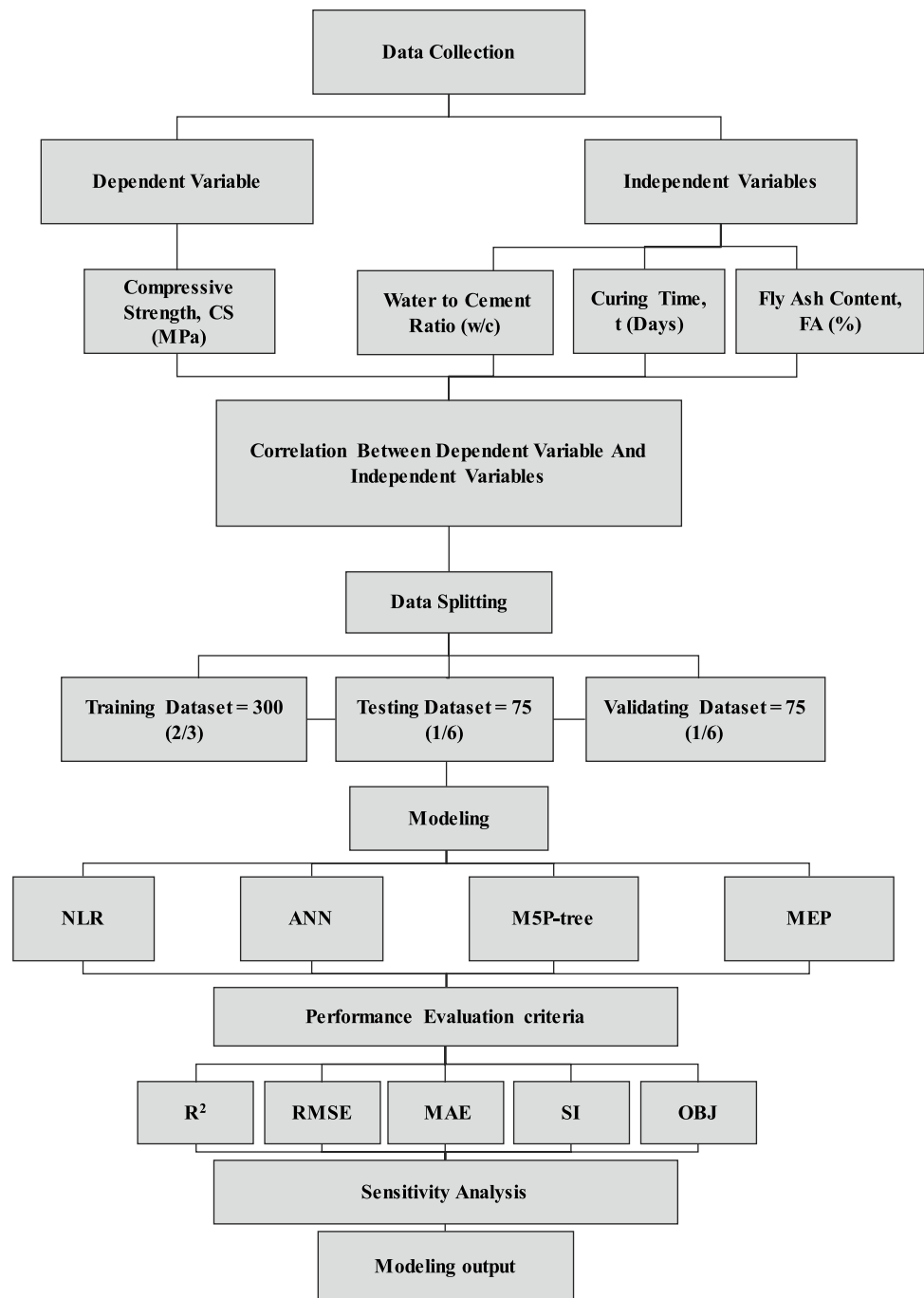
of statistical analysis on the input and output parameters with detail of the collected data is shown in Table 1.

## 3.2 Statistical Analysis

(i) Water to cement ratio (w/c)

According to the statistical evaluation on the collected data, w/c was ranged between 0.24 to 1.2, with mean, Standard Deviation (SD), Variance (Var), Skewness (Skew), and Kurtosis (Kur) of 0.44, 0.18, 0.03, 1.34, 3.32, respectively.

The relation between w/c and compressive strength and the histogram for w/c is shown in Fig. 2a.

(ii) Curing time (t), (days)

The collected dataset contained experimental results from previous studies; the curing time ranged from 1 to 360 days, with a median of 7 days, SD, Var, Skew, and Kur of 51 days, 2672.98 4.19, 21.64, respectively. The histogram for curing time and variation of compressive strength with curing time are presented in Fig. 2b.

(iii) Fly ash content, FA (%)

**Table 1** Summary of statistical analysis of model input parameters

| References | Water to cement ratio (w/c) | Curing time, t (Days) | Fly ash content, FA (%) | Compressive strength,CS (MPa) | Flexural strength, FS (MPa) | Splitting tensile strength, STS (MPa) |
|---|---|---|---|---|---|---|
| [24] | 0.30–1.2 | 1, 3, 7, 28, 90, and 360 | 0–50 | 16–55 | – | – |
| [25] | 0.5 | 7, 28, and 90 | 0–25 | 10–32 | – | 1.5–4 |
| [26] | 0.48 | 7, 14, 28, 56, and 90 | 0–55 | 3.9–30 | – | 1.2–3 |
| [27] | 0.5– 0.58 | 28 | 0–18 | 7–12 | – | – |
| [28] | 0.46 | 1, 3, 7, and 28 | 0–40 | 7–60 | 2–8 | – |
| [29] | 0.3 | 28, and 90 | 0–55 | 70–81 | 5–14 | 1.5–3.8 |
| [20] | 0.5–0.62 | 7, 28, 90 | 0–20 | 29–56 | – | – |
| [30] | 0.4–0.49 | 3, 7, 28, 90 | 30 and 55 | 16–37 | – | – |
| [31] | 0.44 | 3, 7, 28, 50 | 0–30 | 23–54 | – | – |
| [32] | 0.5 | 7, 28 | 0–50 | 26–40 | 3–7 | – |
| [33] | 0.5 | 2, 7, 28 | 30 | 19–50 | – | – |
| [34] | 0.5 | 1, 28, 90 | 0–35 | 12–72 | 3–9 | – |
| [35] | 0.32–0.38 | 28 | 10 | 45–84 | – | – |
| [36] | 0.56 | 7, 28, 90 | 0–20 | 23–43 | 4–7 | – |
| [37] | 0.24–0.8 | 1, 3, 7, 14, 90 | 0–35 | 12–60 | 3–8 | – |
| [38] | 0.5 | 7, 14, 28 | 0–7 | 19–31 | – | – |
| Min | 0.24 | 1 | 0 | 3.9 | 2 | 0.4 |
| Max | 1.2 | 360 | 55 | 84 | 14 | 4 |
| Mean | 0.44 | 28 | 6.77 | 32.94 | 6.13 | 2.65 |
| SD | 0.18 | 51 | 11.87 | 14.02 | 1.878 | 0.836 |

Based on the collected data from the literature, the maximum percentage of cement replacement with fly ash was 55%. With a mean, SD, Var, Skew, and Kur of 6.77%, 11.87, 140.97, 1.76, 2.13, respectively. The variation of compressive strength with the percentage of the replacement of fly ash content and histogram for fly ash content is displayed in Fig. 2c.

(iv) Compressive strength (CS)

From 450 datasets, the compressive strength of cement-based mortar modified with fly ash up to 360 days was ranged from 3.9 to 84 MPa, with a median of 30.3 MPa, SD, Var, Skew, and Kur of 14.02 MPa, 196.59, 0.57, and 0.18, respectively. The histogram of compressive strength of cement-based mortar modified with fly ash and Weibull Distribution Function is shown in Fig. 3a.

(v) Flexural strength (FS)

Based on 56 data of the tested sample collected from literature, flexural strength for cement-based mortar up to 360 days was ranged from 0.5 to 8.5 MPa, with a Median of 6.8, SD, Var, Skew, and Kur of 1.88 MPa, 3.526,–1.01, and–0.394, respectively. The histogram for flexural strength and smallest extreme value distribution function is shown in Fig. 3b.

(vi) Splitting tensile strength (STS)

According to the 26 data collected from previous research about fly ash modified cement-based mortar up to

360 days, the splitting tensile strength was varied from 1.2 to 4 MPa, with a median of 2.77 MPa. SD, Var, Skew, Kur of 0.837 MPa, 0.7, − 0.228, -1.1212, respectively. The histogram for splitting tensile strength with the smallest extreme value distribution function is displayed in Fig. 3c.

## 3.3 Modeling

From the correlation between independent variables and dependent variable direct relationship between cement-based- mortar compositions and compressive strength were not observed; as can be seen from the correlation matrix (Fig. 4), the correlation coefficient (R) of CS with w/c, curing time, and fly ash content are − 0.386, 0.541, − 0.279, respectively. Accordingly, the relations are poor between dependent and independent variables, which means that the compressive strength of the cement-mortar is a multivariable function. Therefore, MEP is used to develop a model to predict the compressive strength of cement-based mortar modified with fly ash based on the cement-mortar composition such as w/c, curing time, and fly ash content.

### 3.3.1 Multi-Expression-Programing (MEP Model)

Genetic Algorithm (GA) was first introduced by Holland [40], which was motivated through evolution theory, similar to that

**Fig. 2** Marginal plot for **a** compressive strength (CS) with water to cement ratio, **b** CS with curing time, and **c** CS with fly ash content
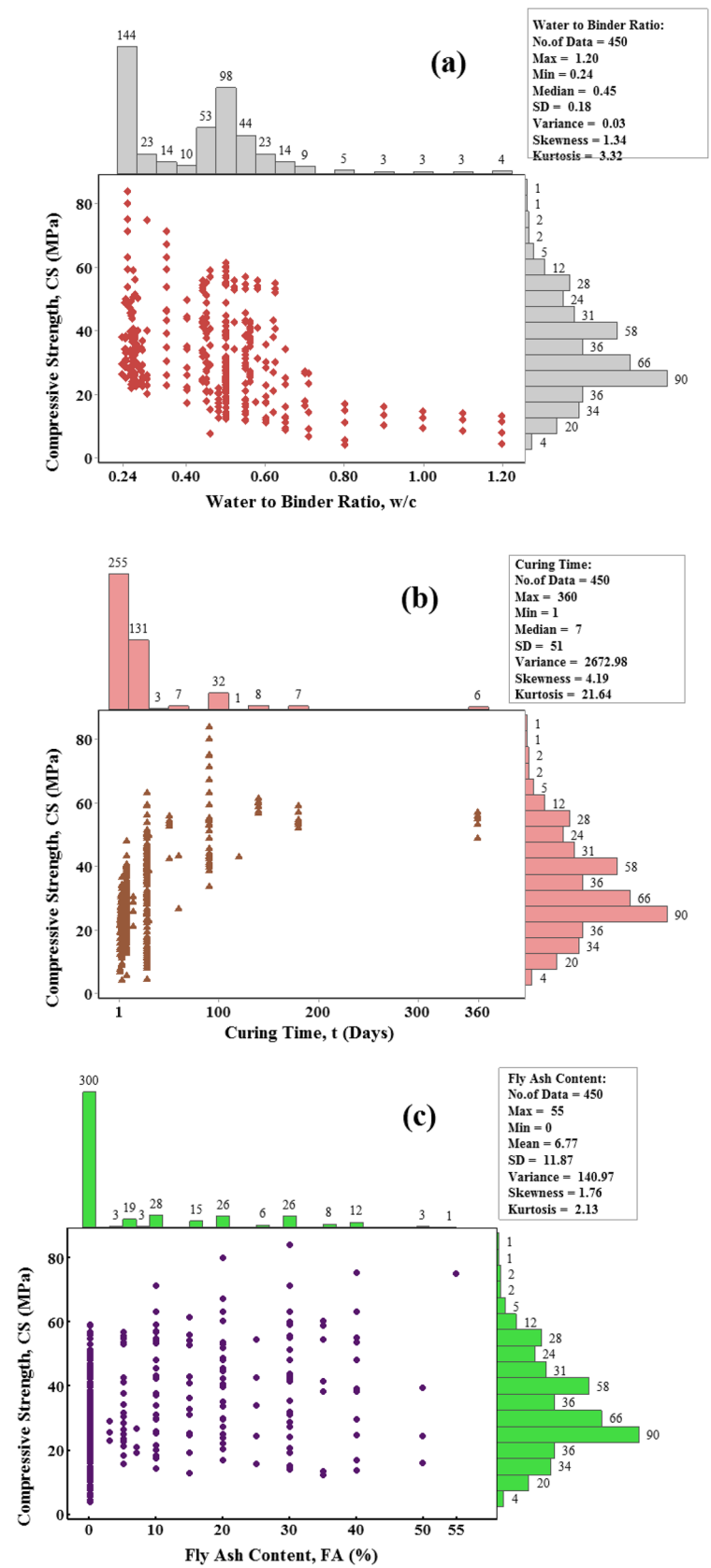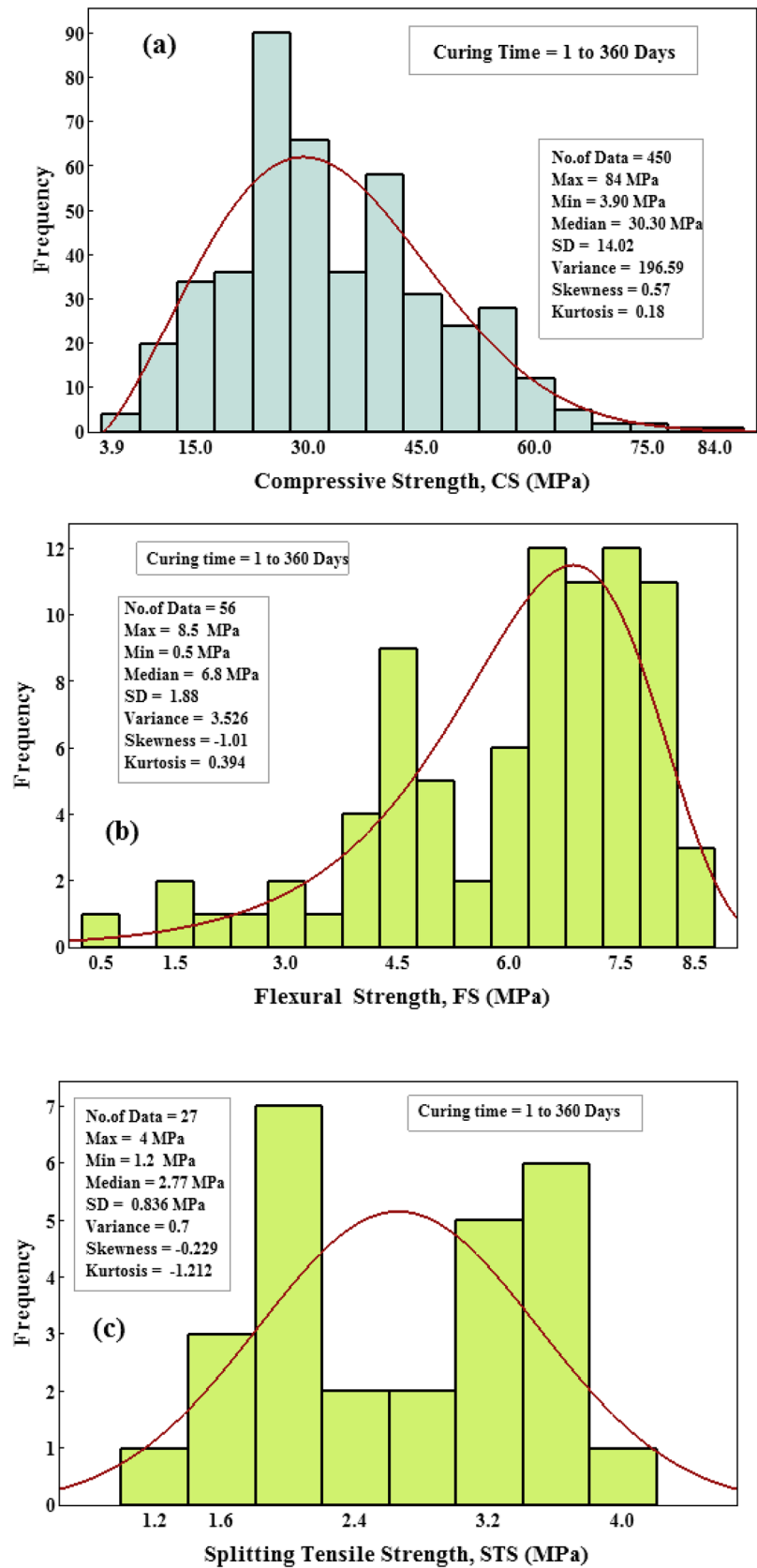
**Fig. 3** Histogram for **a** compressive strength, **b** flexural strength, and **c** splitting tensile strength for fly ash modified cement mortar from 1 to 360 days of curing
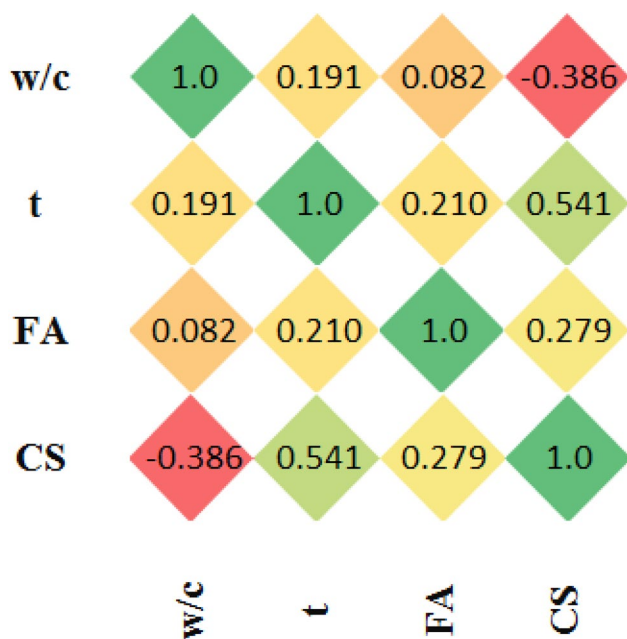
**Fig. 4** Correlation matrix for independent variables and dependent variable

**Table 2** Optimal parameters for MEP model

| Parameters | Setting |
| --- | --- |
| Subpopulations number | 50 |
| Subpopulation size | 200 |
| Code length | 50 |
| Probability of crossover | 0.9 |
| Mathematical operator | $+, -, *, /$ |
| Probability of alteration | 0.01 |
| Competition size | 4 |
| Functions probability | 0.5 |
| Variables probability | 0.5 |
| Generations | 1000 |

of Genetic Programming (GP) proposed by Cramer [40–42]. Several linear variations of GP have already been proposed to deal with some difficulties (such as bloat) caused by tree representations of GP. A few examples are Cartesian Genetic Programming, Grammatical Evolution (GE), Linear GP, and Gene Expression Programming [43]. MEP individuals are strings of genes encoding complex computer programs; when MEPs package expressions for conceptual regression issues, they comparably represent them to how processors convert C or Pascal expressions into machine code [44]. Multiple solutions are stored in a separate chromosome in MEP individuals. The most acceptable option is generally chosen. This is known as strong implicit parallelism, and it is a distinctive characteristic of MEP [45, 46]. This feature does not make MEP more complex when compared with GE and GEP. The MEP model incorporates different fitting factors to generate a generalized relationship. Simple math operators were employed to generate simple expressions in this investigation, and a trial-and-error procedure was used to determine the fitting parameters [47], as presented in Table 2.

### 3.3.2 Nonlinear Regression Model (NLR)

The following formula can be considered a general form for developing a nonlinear regression model [39, 48] to predict the compressive strength from the cement-mortar components, including the FA content (Eq. 1).

$$CS = \beta_1 \left(\frac{w}{c}\right)^{\beta_2}(t)^{\beta_3} + \beta_4 \left(\frac{w}{c}\right)^{\beta_5}(t)^{\beta_6}(FA)^{\beta_7} \quad (1)$$

CS, w/c, t, and FA are compressive strength, water to cement ratio, curing time, fly ash content, and $\beta_1$ to $\beta_7$ are model parameters.

### 3.3.3 ANN Model

ANN is the computing system designed to simulate the way how the human brain processes and analyses. Also, this model is a machine learning system used for various numerical predictions/problems in Construction Engineering. ANN includes the input layer, the hidden layer (one or more layers), and the output layer. The hidden layer is related by weight, transfer function, and bias to the other layers. A multi-layer feed-forward network was programmed with a mixture of proportions, w/b, curing time, and FA content like inputs, and compressive strength as output. There is no standard method for designing or selecting a network architecture. Therefore, the maximum number of hidden layers and neurons was calculated by the trial and error test based on the lowest average square error criterion. The second step of the optimal network design process was to choose the optimum number of epochs during the training that gave the minimum MAE and RMSE and high R-value. The same preliminarily designed networks with hyperbolic tangent transfer functions were used to see the effect of several epochs on reducing the MAE and RMSE. The MAE variations with the number of epochs are presented for the preliminarily designed networks. After designing the optimum architecture, the available data set (total of 450 data) was divided into two parts; the first part was 2/3 of the overall data set (300) for training the network, the second part was 1/3 of the total data set (150) for testing and validating the network [17]. Several transfer functions and ANN structures with a varied number of hidden layers and neurons were
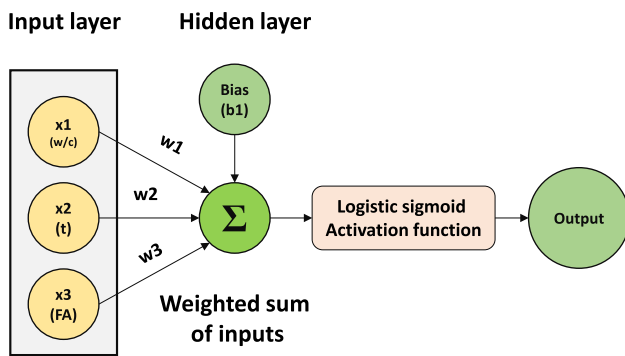
**Input layer** **Hidden layer**



Fig. 5 Typical procedure for output of ANN network in a single node

**Table 3** Model parameters for M5P-tree model

| LM | $CS = a + b\left(\frac{w}{c}\right) + c(t) + d(FA)$ | | | |
|---|---|---|---|---|
| | Model Parameters | | | |
| | a | B | c | d |
| 1 | 37.420 | − 53.972 | 1.942 | 0.196 |
| 2 | 36.267 | − 38.455 | 0.601 | 0.001 |
| 3 | 29.691 | − 18.188 | 0.521 | − 0.102 |
| 4 | 58.951 | − 51.344 | 0.096 | 0.241 |

tested to design the optimal network structure to predict the cement mortar compressive strength. Among the networks, one hidden layer with seven neurons and a hyperbolic tangent transfer function were chosen due to having the minimum mean absolute error (MAE) (Fig. 9). In this part of the research, the ANN model was used to estimate the compressive strength of FA-containing cement mortar as a cement replacement, w/b, curing time, and FA contents.

The Artificial Neural Network (ANN) is a computing system that resembles the human brain and its information analysis. In addition, this model is a machine learning system employed in construction engineering for various numerical forecasts and difficulties [49]. ANN consists of three layers input, hidden, and output layer; these layers are connected through biases and weights. The behavior of an ANN network is influenced by the connections of neurons pattern, which also determines the class of the network. It is possible to train a network to enhance network performance. In more technical terms, the topology of the network and connection weights change repeatedly such that the error at each output layer node is minimized [21]. In this study, a multi-layer feed-forward network was designed with mortar composition (w/c, t, FA) as input and CS as output, and a sigmoid activation function is used in the output layer.

$$Output = f\left(\sum_{j=1}^{n} w_j x_j + bias\right) \qquad (2)$$

where j is the number of input variables, $x_j$ is the input number j, and bias is the threshold for sigmoid activation function. The typical process of the result of ANN is illustrated in Fig. 5.

### 3.3.4 M5P-Tree Model

Quinlan [50] first devised the M5 algorithm, which was developed into the M5P-tree algorithm [51]. One of the most significant advantages of model trees is their ability to efficiently solve problems, dealing with many data sets with

a substantial number of attributes and dimensions. They are also noted for being powerful while dealing with missing data. The M5P-tree approach establishes a linear regression at the terminal node by classifying or partitioning diverse data areas into numerous separate spaces. It fits on each sublocation in a multivariate linear regression model. The error is estimated based on the default variance value inserted into the node. The general formula for the M5P-tree model is shown in Eq. 3.

$$CS = a + b\left(\frac{w}{c}\right) + c(t) + d(FA) \qquad (3)$$

CS, w/c, t, and FA are compressive strength, water to cement ratio, curing time, fly ash content, and a, b, c, and d are model parameters (Table 3).

### 3.3.5 Correlation of Compressive Strength with Flexural and Splitting Tensile Strengths

(i) Vipulanandan Correlation Model

A Vipulanandan correlation model was used to develop the relationship between CS and FS of cement mortar modified with fly ash [16, 52–57]. The model is displayed in Eq. 4.

$$FS\ or\ STS = \frac{CS}{a + b(CS)} \qquad (4)$$

FS, STS, and CS are flexural strength, splitting tensile strength, and compressive strength.

a & b are model parameters. The performance of the Eq. 4 was compared with the following models (Eqs. 5, 6, and 7).

(ii) Exponential Association 2 model

The Exponential Association 2 model is also used to correlate the flexural strength with the compressive strength of cement-based mortar; the model is shown in Eq. 5 [58, 59].

$$FS = \propto \left(1 - e^{-\beta(CS)}\right) \qquad (5)$$

FS, CS are flexural and compressive strengths, α & β are model parameters.

(iii) DR-Hill-Zero background model

Additionally, the DR-Hill-Zero background model is used to predict flexural and splitting tensile strengths from compressive strength, which is displayed in Eq. 6 [60].

$$FS \, or \, STS = \frac{\theta(CS)^{\eta}}{\kappa^{\eta} + (CS)^{\eta}} \tag{6}$$

FS, STS, and CS are flexural strength, splitting tensile strength, and compressive strength. θ, η, and κ are model parameters.

(iv) Power Model

The power model formula is presented in Eq. 7 [61].

$$FS \, or \, STS = \varphi(CS)^{\omega} \tag{7}$$

FS, STS, and CS are flexural strength, splitting tensile strength, and compressive strength. φ and ω and are model parameters.

## 4 Performance criteria for model evaluation

The developed models are evaluated based on different assessment tools to choose the best model to predict the CS of the mortar; the following are efficiency measurements for the models:

$$R^2 = 1 - \frac{\sum_1^n (yp - ye)^2}{\sum_1^n \left(ye - \overline{ye}\right)^2} \tag{8}$$

$$R = \sqrt{R^2} \tag{9}$$

$$RMSE = \sqrt{\frac{SSE}{n}} \tag{10}$$

$$MAE = \frac{\sum_1^n |yp - ye|}{n} \tag{11}$$

$$MBE = \frac{\sum_1^n (yp - ye)}{n} \tag{12}$$

$$SI = \frac{RMSE}{\overline{ye}} \tag{13}$$

$$OBJ = \left(\frac{n_{tr}}{n_{to}} * \frac{RMSE_{tr} + MAE_{tr}}{R^2_{tr} + 1}\right) + \left(\frac{n_{te}}{n_{to}} * \frac{RMSE_{te} + MAE_{te}}{R^2_{te} + 1}\right) + \left(\frac{n_{val}}{n_{to}} * \frac{RMSE_{val} + MAE_{val}}{R^2_{val} + 1}\right) \tag{14}$$

$$t-_{test} = \sqrt{\frac{(n-1)MBE^2}{RMSE^2 - MBE^2}} \tag{15}$$

$$U_{95} = 1.96 * \sqrt{SD^2 + RMSE^2} \tag{16}$$

$$\rho = \frac{SI}{1 + R} \tag{17}$$

where $R^2$, RMSE, MAE, MBE, SI, OBJ, t-test, $U_{95}$, and ρ are Coefficient of Determination, Root Mean Squared Error, Mean Absolute Error, an Average of Errors, Scatter Index, Objective, t-test, 95% Confidence Uncertainty, and Performance Index, respectively. yp, ye, and $\overline{ye}$ are predicted compressive strength, measured compressive strength, and an average of measured compressive strength, respectively. n, tr, te, val. are several data in the training, testing, and validating dataset.

For all of the assessment parameters, the ideal value is zero, while the best value for $R^2$ is 1. Corresponding to SI, the performance of the model is excellent, good, fair, and poor if the SI < 0.1, 0.1 < SI < 0.2, 0.2 < SI < 0.3, and SI > 0.3, respectively [62].

## 5 Analysis of outputs

### 5.1 Relation between predicted and measured compressive strength

#### 5.1.1 MEP model

Comparison of measured with the predicted value of CS using the MEP model is presented in Fig. 6. The model had a good performance with $R^2$ of 0.87, 0.87, and 0.897 for training, testing, and validating, respectively. Figure 6a contained -20 and +25% error lines in the training phase and -10 and 15% for testing and validating (Fig. 6 b &c).

$$CS = A + B + C + 25 - \frac{D - B - C - 25}{D + \frac{2}{3}} - E - \frac{B + C}{F} \tag{18a}$$

$$A = \frac{2\left(\frac{w}{c}\right)(FA)}{25} - 15\left(\frac{w}{c}\right)^2 \tag{18b}$$

$$B = \frac{2}{15(t - 15\left(\frac{w}{c}\right)^2)} \tag{18c}$$

$$C = \frac{2(FA)}{15(\frac{w}{c})} \tag{18d}$$

**Fig. 6** Variation of CS Predicted with CS Measured using MEP model **a** training data, **b** testing data, and **c** validating data
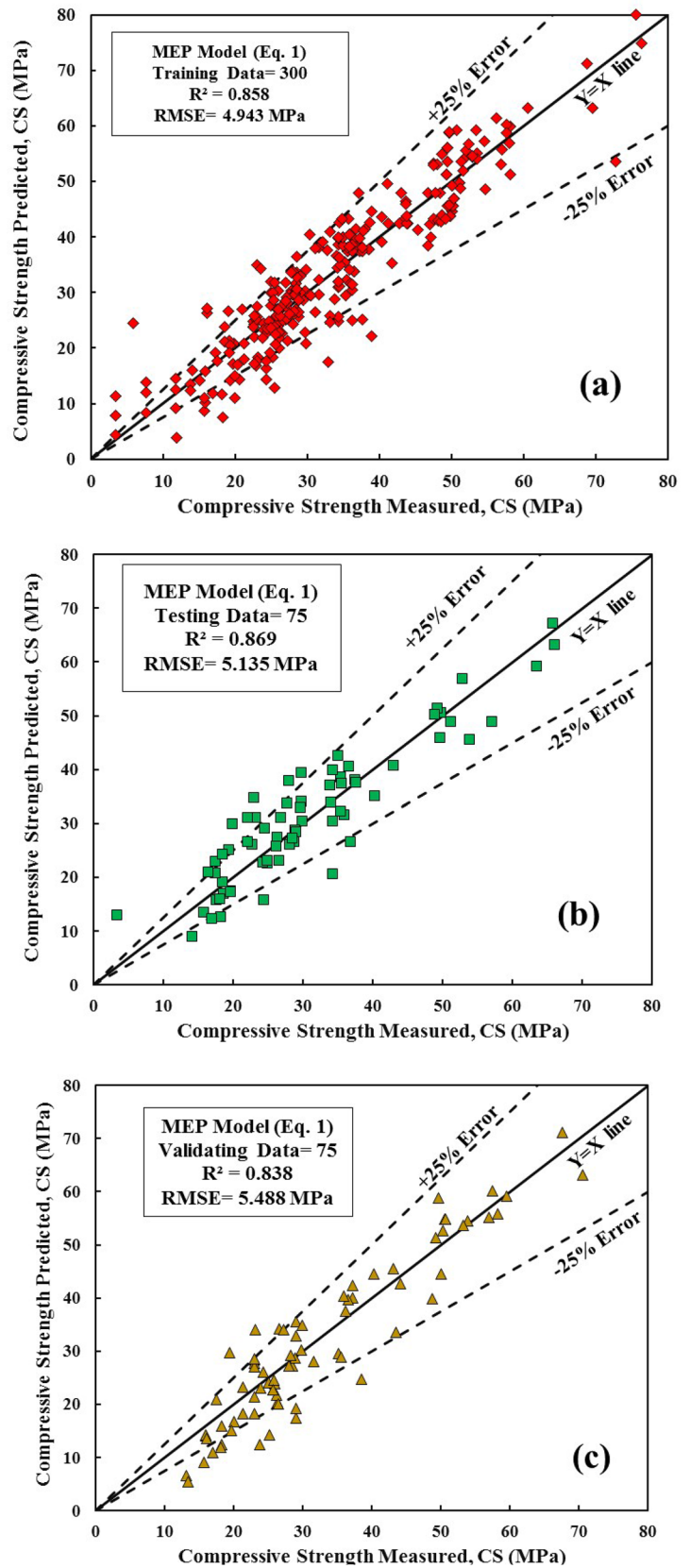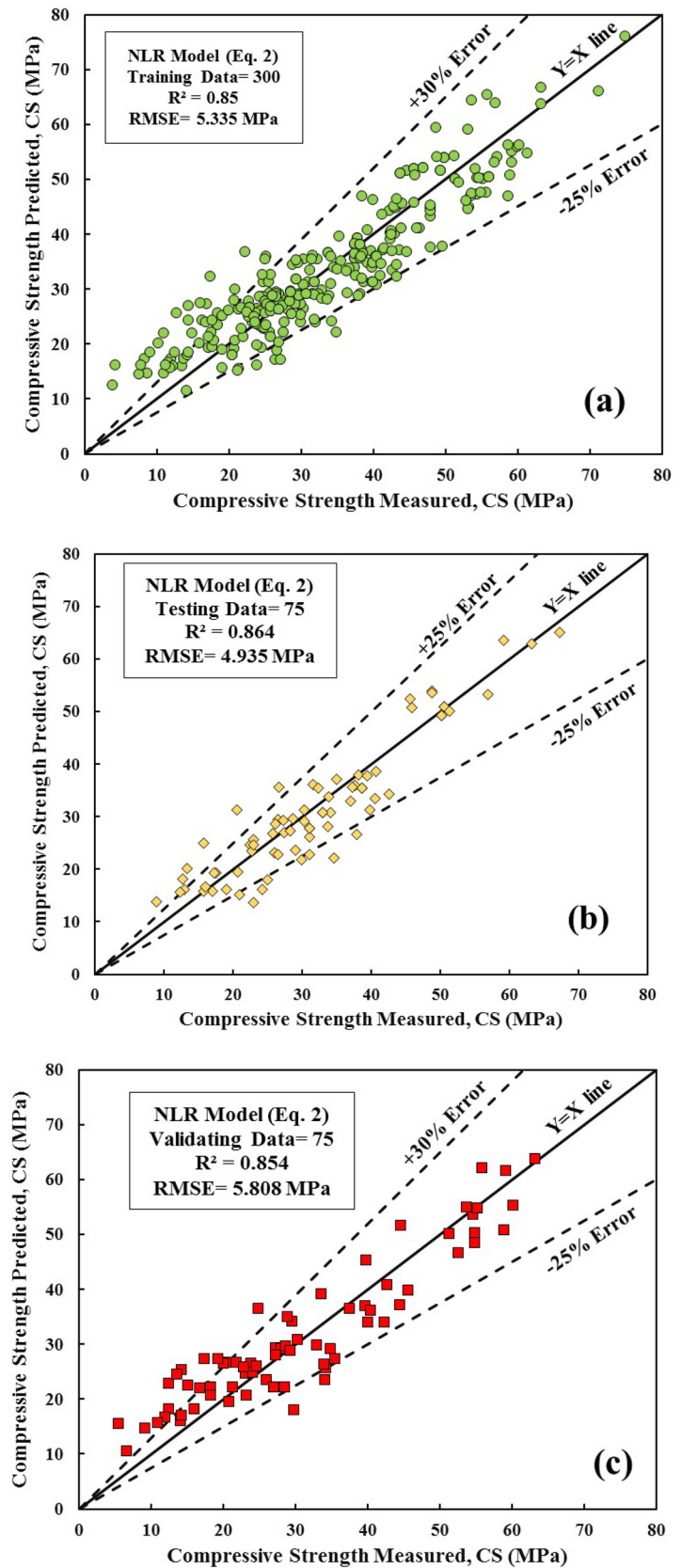
**Fig. 7** Variation of CS Predicted
with CS Measured using NLR
model **a** training data, **b** testing
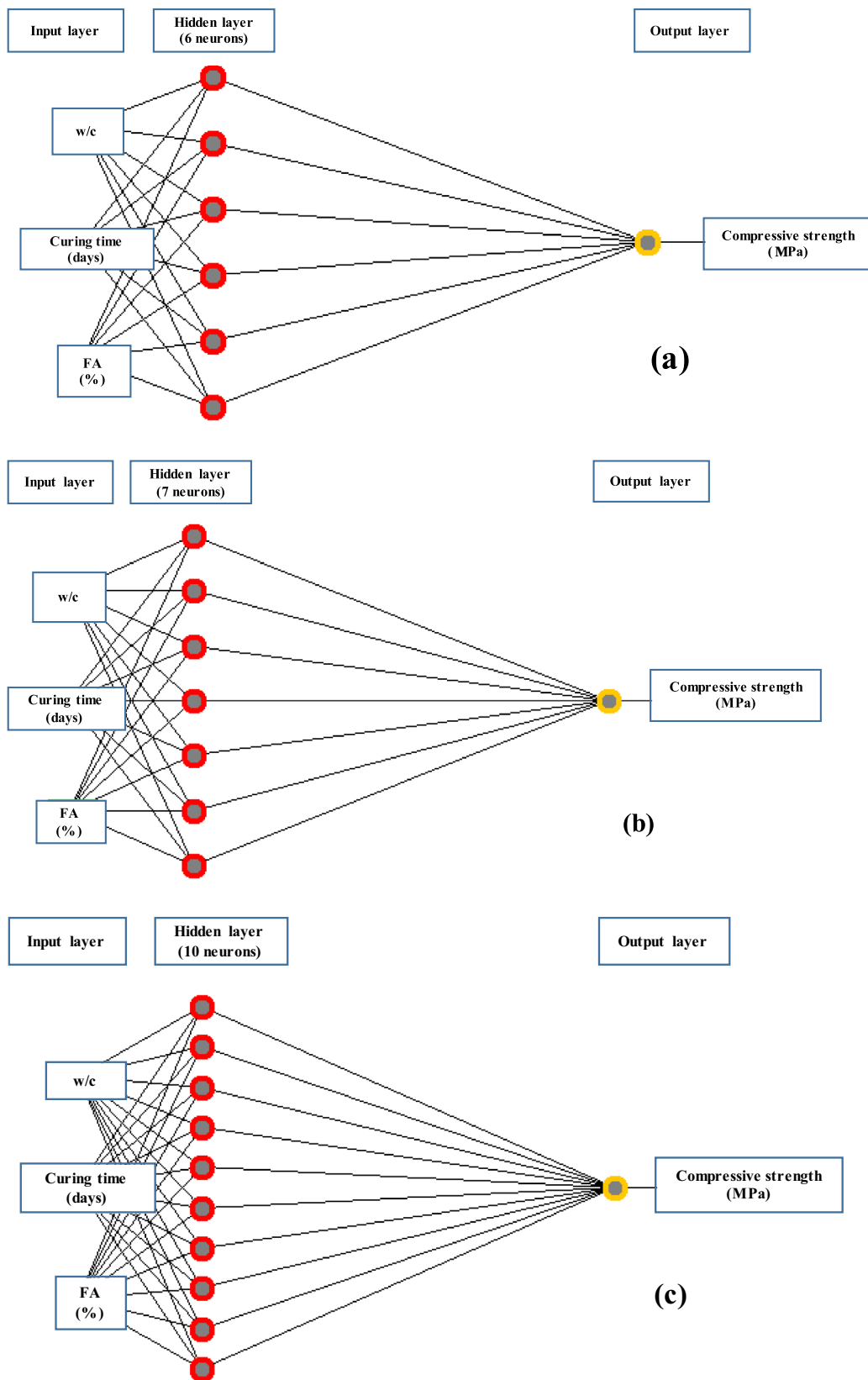data, and **c** validating data

**Fig. 8** Optimal ANN network structures **a** one hidden layer and 6 hidden neurons, **b** one hidden layer and 7 hidden neurons, and **c** one hidden layer and 10 hidden neurons
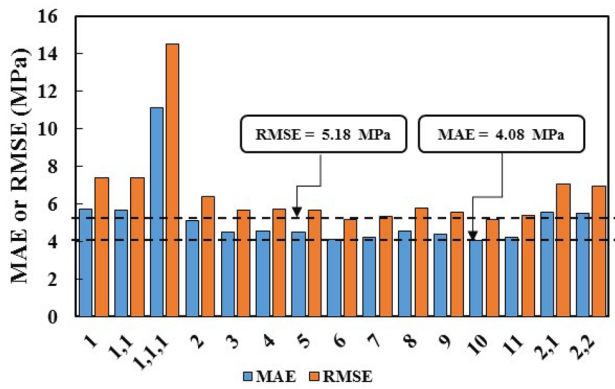
**Fig. 9** Optimal ANN network selection based on RMSE and MAE

$$D = \frac{225(\frac{w}{c})^2}{2(t - 15(\frac{w}{c})^2} \tag{18e}$$

$$E = \frac{4(FA)^2}{375} \tag{18f}$$

$$F = 225(\frac{w}{c})^3 \tag{18g}$$

No. of Data = 300, $R^2$ = 0.858, RMSE = 4.943 MPa.

### 5.1.2 NLR Model

The variation of predicted compressive strength with measured compressive strength is displayed in Fig. 7. From the modeling result, it is clear w/c and curing time are affect the CS more than fly ash content. In comparison, the effect of w/c is more significant on the compression strength of cement-mortar. The model is developed, and the parameters are determined using the least square method and solver technique [63]. The NLR model is presented in Eq. 18.

$$CS = 0.62 \times \frac{(t)^{0.273}}{\left(\frac{w}{c}\right)^{0.872}} \times (FA)^{0.208} + 7.681 \times \frac{(t)^{0.235}}{\left(\frac{w}{c}\right)^{0.759}} \tag{19}$$

No. of Data = 300, $R^2$ = 0.85, RMSE = 5.34 MPa.

### 5.1.3 ANN Model

Figure 8 shows the optimal ANN network structures, the best network structure (Fig. 8) selected containing one hidden layer and six hidden neurons, with momentum, learning rate, learning time of 0.1, 0.2, and 2000, respectively. Those mentioned parameters for the network were determined by trial and error based on RMSE and MAE, as illustrated

in Fig. 9. Figure 10 shows variation in predicted CS with measured CS using the training dataset and error line -20 to +20%, indicating the measurements and predictions are in this limit with $R^2$, RMSE of 0.859, and 5.179 MPa.

#### 5.1.4 M5P-Tree Model

Figure 11 shows the division of the input space by the algorithm of the M5P-tree model into four linear regression functions named LM 1 and LM 4. The relationship of predicted and measured CS of the M5P-tree model showed in Fig. 12, with $R^2$ and RMSE of 0.824 and 5.771 MPa. There are -20 to 25% error lines for the training data set and -15 to 20% for testing, and -15 to 25% for validating datasets. Figure 11 shows the pruned M5P-tree, which classified the training dataset into four parts based on the criteria shown in the figure; each part of the divided dataset resulted in a single regression model as mentioned in Eq. 3, the model parameters for the M5P-tree model are summarized in Table 3.

### 5.2 Relationship Between Compressive, Flexural, and Tensile Strengths

Based on the collected data, three different models were developed to predict flexural and splitting tensile strengths from measured compressive strength using the Vipulanandan correlation model, Exponential association-2, DR-Hill-Zero background, and Power model, as illustrated in Eqs. 20 to 25. Figure 13a shows the variation of FS with CS for data collected from literature and predicted FS using developed models. The residual error for predicted FS from CS ranged between 1 to −1 MPa is shown in Fig. 13b. Variation of splitting tensile strength with CS is shown in Fig. 13c, and the residual errors for predicted STS from CS using ranged between 0.15 to −0.35 MPa (Fig. 13d).

(v) Vipulanandan correlation model

$$FS = \frac{CS}{3.06 + 0.073(CS)} \tag{20}$$

No. of data = 56, $R^2$ = 0.955, RMSE = 0.396 MPa

$$STS = \frac{CS}{5.144 + 0.108(CS)} \tag{21}$$

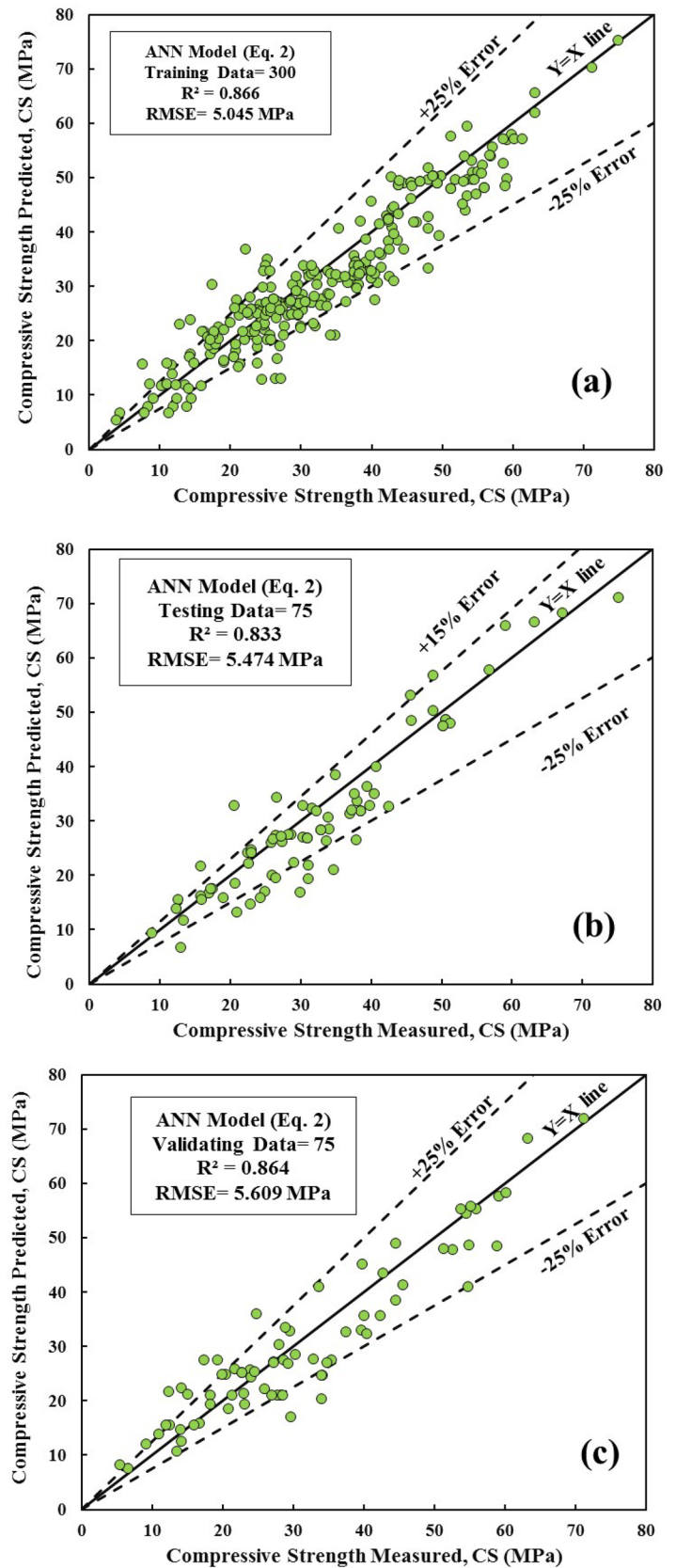No. of data = 27, $R^2$ = 0.981, RMSE = 0.115 MPa.
(vi) Exponential association 2

$$FS = 9.446(1 - e^{-0.032(CS)}) \tag{22}$$

No. of data = 56, $R^2$ = 0.958, RMSE = 0.386 MPa.
(viii) DR-Hill-Zero Background

**Fig. 10** Variation of CS Predicted with CS Measured using ANN model **a** training data, **b** testing data, and **c** validating data
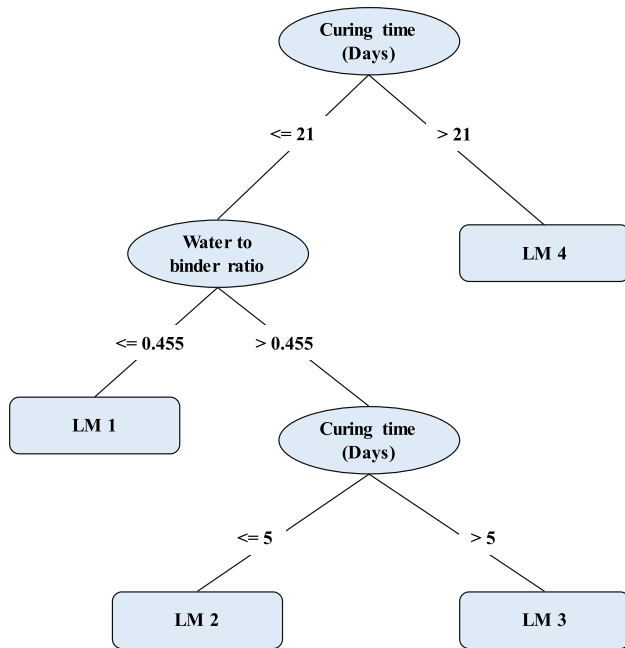
**Fig. 11** Pruned M5P-tree model

$$FS = \frac{10.789(CS)^{1.293}}{26.574^{1.293} + (CS)^{1.293}} \qquad (23)$$

No. of Data = 56, $R^2$ = 0.958, RMSE = 0.382 MPa

$$STS = \frac{71.87(CS)^{0.741}}{1598.864^{0.741} + (CS)^{0.741}} \qquad (24)$$

No. of Data = 27, $R^2$ = 0.982, RMSE = 0.11 MPa.
(viii) Power Model

$$STS = 0.316(CS)^{0.714} \qquad (25)$$

No. of Data = 27, $R^2$ = 0.982, RMSE = 0.11 MPa.

Based on the $R^2$ and RMSE, the DR-Hill-Zero background model is better than other models for predicting flexural strength from compressive strength; on the other hand, the best model for correlation of splitting tensile strength with compressive strength is DR-Hill-Zero background and Power Models.

## 5.3 Model Evaluations

The proposed models are compared according to the relationship between predicted and measured CS for testing data set; the MEP model had less variation; the plotted data are near the Y = X line, which indicates a minor error in predicted values, as shown in Fig. 14a. Furthermore, the maximum and minimum residual errors for the MEP model were -19 and 18 MPa. Residual error of NLR, ANN, and M5P-tree model was -12 to 14 MPa, -14 to 14 MPa, and -21 to 19 MPa, respectively. The residual error indicates better performance of the NLR model than other developed models, as shown in Fig. 14b. The residual errors for the ANN, M5P-tree, and MEP are provided in Fig. 14c and d.

The SI value of the MEP model, NLR, ANN, and M5P-tree model for the training dataset was 0.148, 0.16, 0.155, and 0.173. When comparing SI value for validating datasets, the SI value for the MEP model is less than NLR, ANN, and M5P-tree model by 8, 6, and 16.5%, respectively. For the testing dataset, the SI value of the MEP model is equal to 0.159 and less than ANN, and M5P-tree model by 10 and 5%, and more significant than the NLR model by 5%, as shown in Fig. 15a.

**Fig. 12** Variation of CS Predicted with CS Measured using M5P-tree model **a** training data, **b** testing data, and **c** validating data
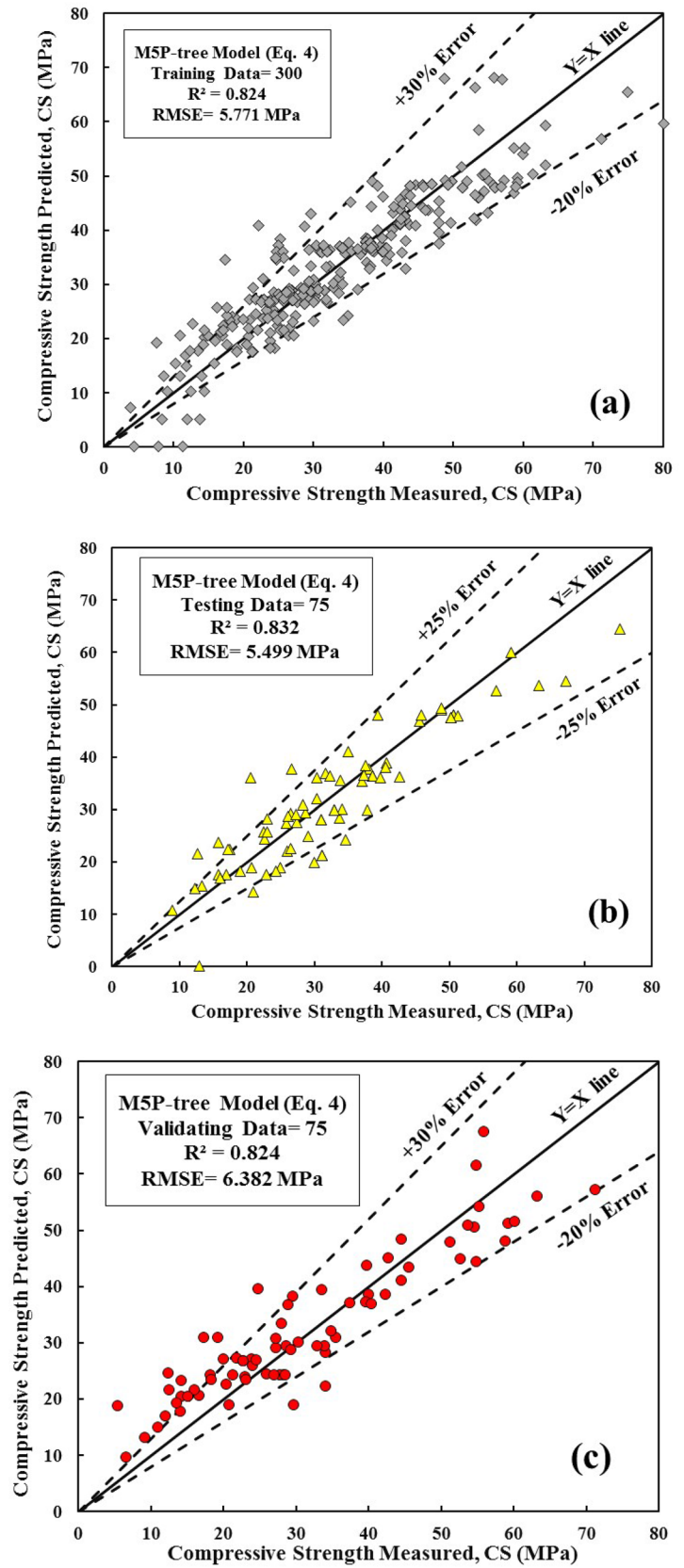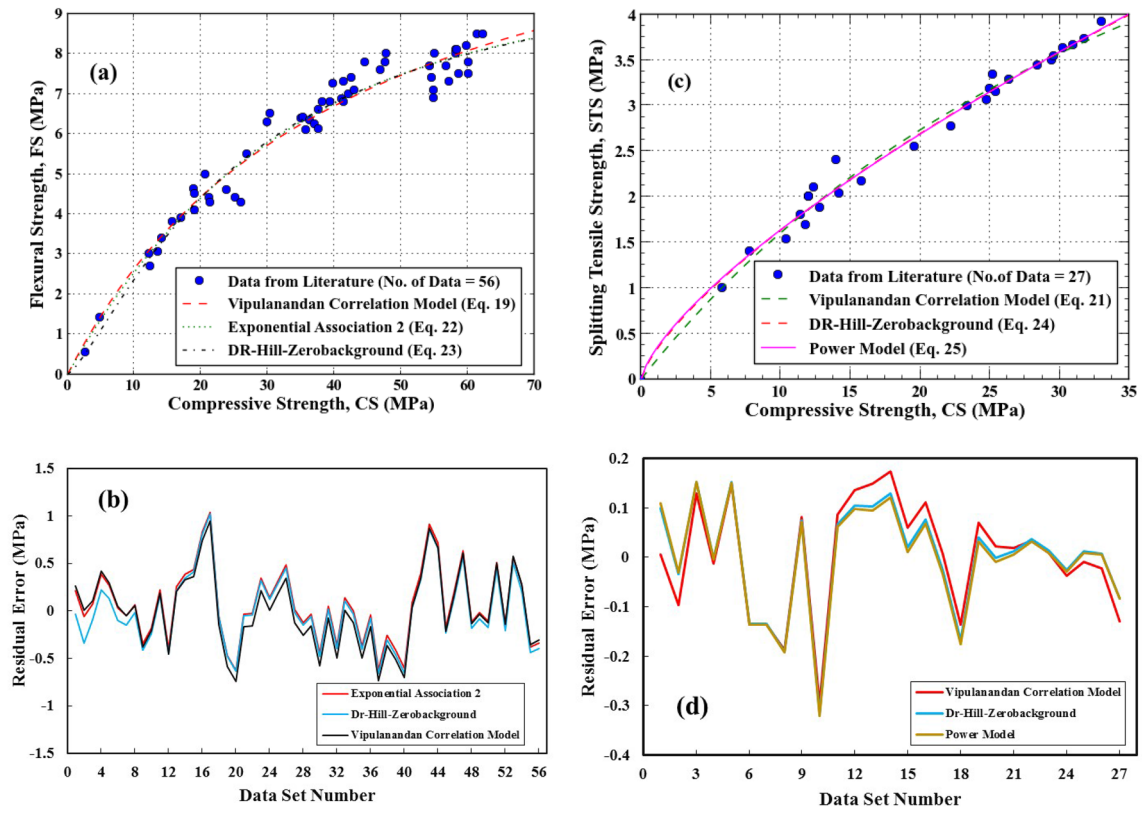
**Fig. 13** Comparing models for flexural strength, splitting tensile strength, and compressive strength correlation using **a** variation of FS with CS, **b** residual error to predict FS, **c** variation of STS with CS, and **d** residual error to predict STS
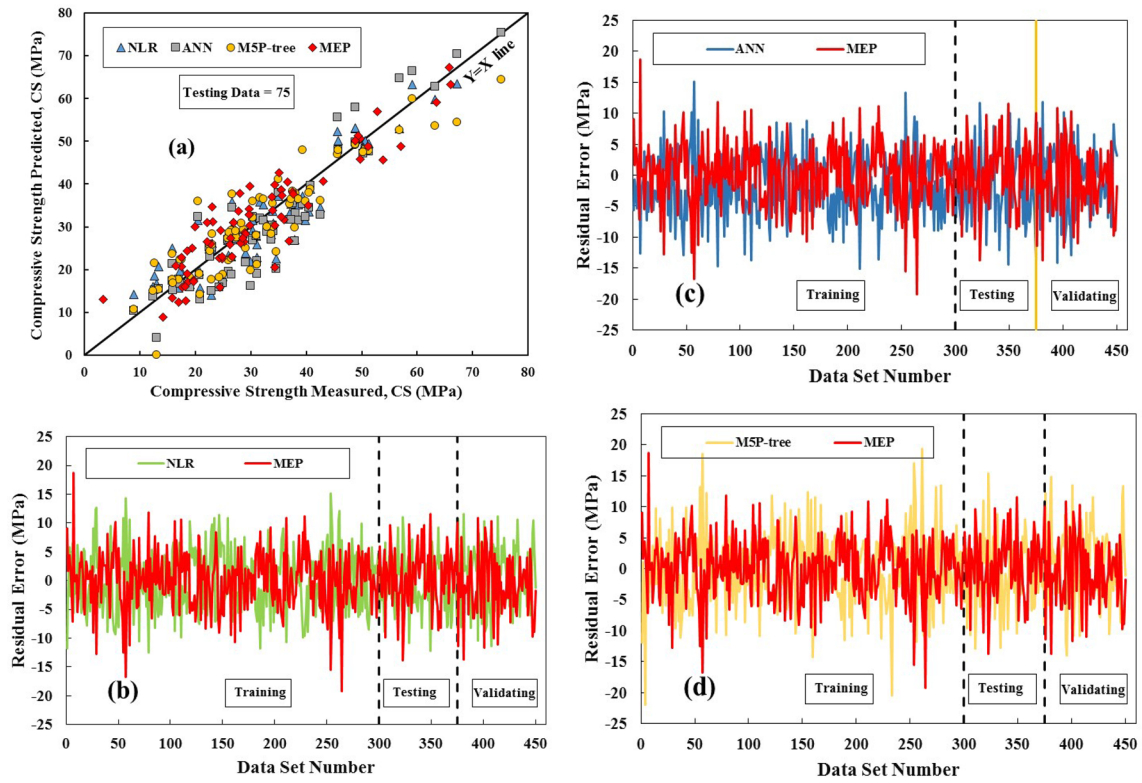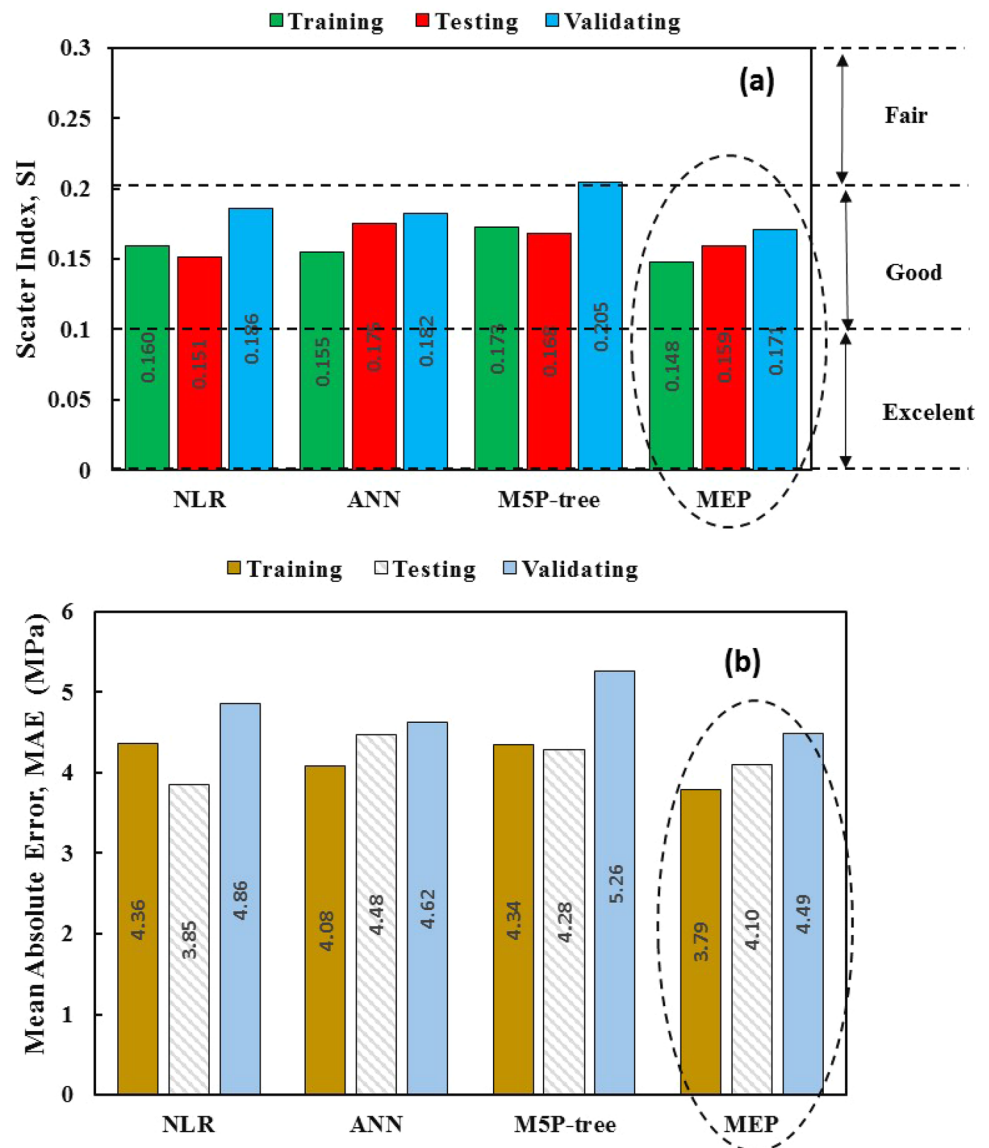
**Fig. 14** Comparison of developed model based on **a** variation between measured and predicted CS values for testing data and **b** residual error for the MEP and NLR models **c** residual error for the MEP and ANN models (d) residual error for the MEP and M5P-tree models

**Fig. 15** Comparing developed models based on **a** SI and **b** MAE



The comparison of developed models based on MAE is presented in Fig. 15b. The MAE for MEP models is less than the MAE of other developed models for training and validating datasets; however, the MAE of MEP model value for testing is less than ANN, and M5P- tree model by 8 and 4%, and greater than the NLR model by 6%.

The OBJ values for the proposed models are also evaluated; the OBJ for the MEP model is less than NLR, ANN, and M5P-tree models by 7, 6, and 14, as displayed in Fig. 16a.

The t-test and $U_{95}$ values comparison for the developed models is illustrated in Fig. 16b. as can be seen from the figure, the uncertainty of the predicted compressive strength for 95% confidence level of MEP model is less than ANN and M5P-tree models by 2 and 6%, and greater than NLR model by 4%. However, the t-test value of the MEP model is less than other developed models. The t-test value results

in a probability of accepting or rejecting the null hypothesis. The larger t-test value indicates a significant difference in the measured and predicted CS of the cement mortar.

Also, the performance index for the MEP model was less than other developed models for training and validating data. At the same time, it is greater than the NLR model in testing the data set by 4%, as presented in Fig. 17.

The box plot for actual and predicted CS is drawn as shown in Fig. 18 (a, b & c). The boxplot for the MEP model had the same pattern for the minimum and maximum CS values, Mean and median. According to the box plot MEP model is better than other developed models.

Summary of model evaluation for $R^2$, RMSE, and MAE of the developed models is presented in Table 4.

**Fig. 16** Comparing developed models based on **a** OBJ and **b** T-stat and U95
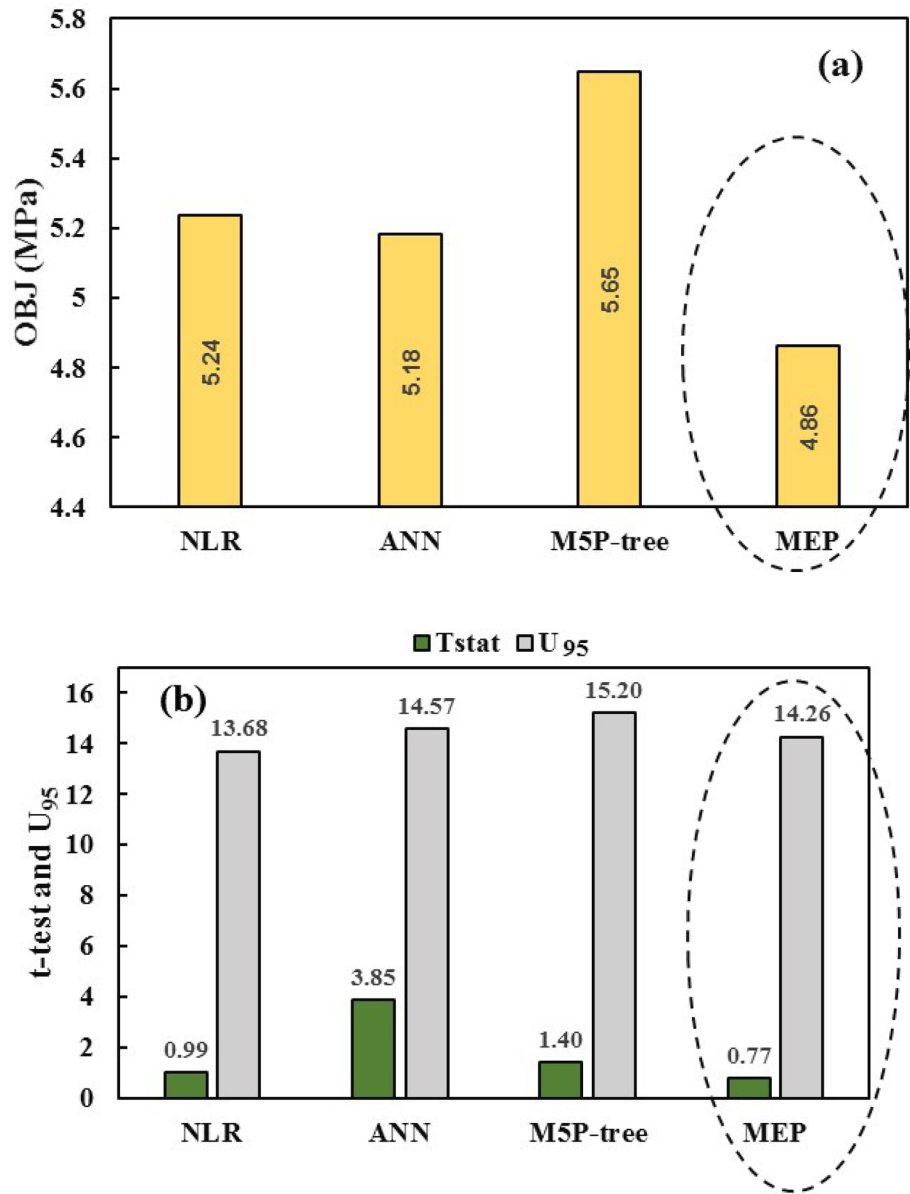


## 5.4 Sensitivity Evaluation

The most influential parameter on the compressive strength of cement-based mortar modified with fly ash is determined using the MEP model. Every time a single input parameter is removed from the training dataset, regression is run again in the process. MAE for the model is recorded, the trial with maximum MAE (MPa) and RMSE (MPa) is chosen, and the trials ranked according to the recorded MAE the more sensitive variable in predicting the compressive strength of cement mortar modified with fly ash is the removed parameter from the trial with the highest MAE. Based on the sensitivity analysis, the most influential parameter is the curing time of the tested samples, as summarized in Table 5.

## 6 Conclusions

Accurate models can be developed using different soft computing techniques; in this study, four different approaches were used to establish a reliable model for the prediction of compressive strength of cement mortar modified with fly ash; the followings are the main conclusion:

1. Based on the collected data from literature maximum percentage of fly ash is 55%, w/c was ranged from

**Fig. 17** Comparing developed models using a performance index
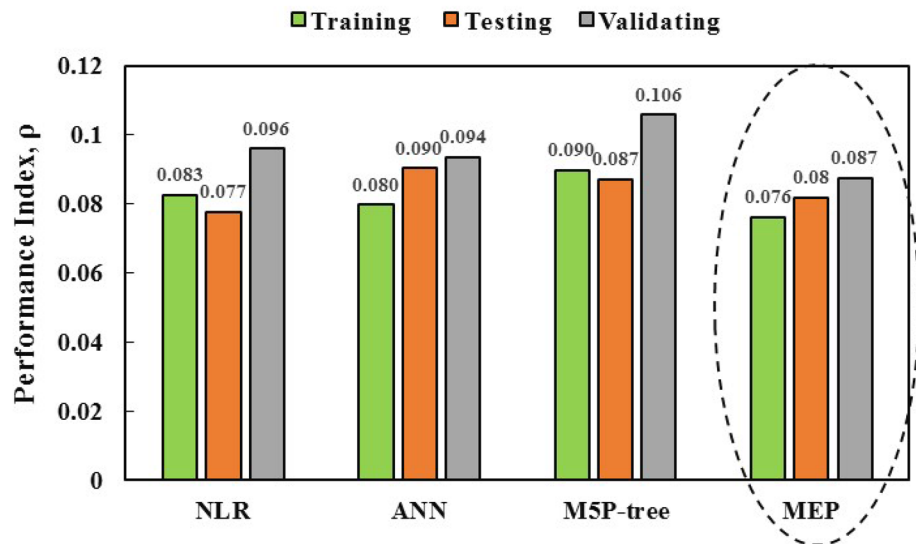


0.24 to 1.2. The addition of fly ash to cement mortar increased the compressive strength for the same mixture and w/c.

2. SI for the MEP model is less than NLR, ANN, and M5P-tree models in training and validating data set; on the other hand, the SI for MEP is more than the NLR model by 5%. The objective value for the MEP model is less than other developed models. 95% Uncertainty ($U_{95}$) value for MEP is smaller than ANN and M5P-tree models. Nevertheless, its $U_{95}$ value is greater than the $U_{95}$ of the NLR model by 4%. t-test value for the MEP model is less than other developed models.

3. The performance index of the MEP model for training and the validating dataset is less than other developed models.

4. Based on the box plot for actual and predicted compressive strength, the MEP model predictions had the same arrangement as real compressive strength compared to other developed models in maximum, minimum, mean, and median.

5. According to the statistical evaluation tools, the MEP model is better than NLR, ANN, and M5P-tree models for compressive strength prediction. It has less scatter in predicted compressive strength compared with measured compressive strength.

6. Depending on the sensitivity evaluation result, the curing time of the sample is the most influential parameter on the compressive strength of cement mortar modified with fly ash.

7. Reliable nonlinear models were used to predict the splitting tensile strength and the flexure strength of cement mortar modified with FA with a minimal prediction error.

**Fig. 18** Comparing developed models using boxplot for actual and predicted compressive strength values **a** training data, **b** testing data, and **c** validating data
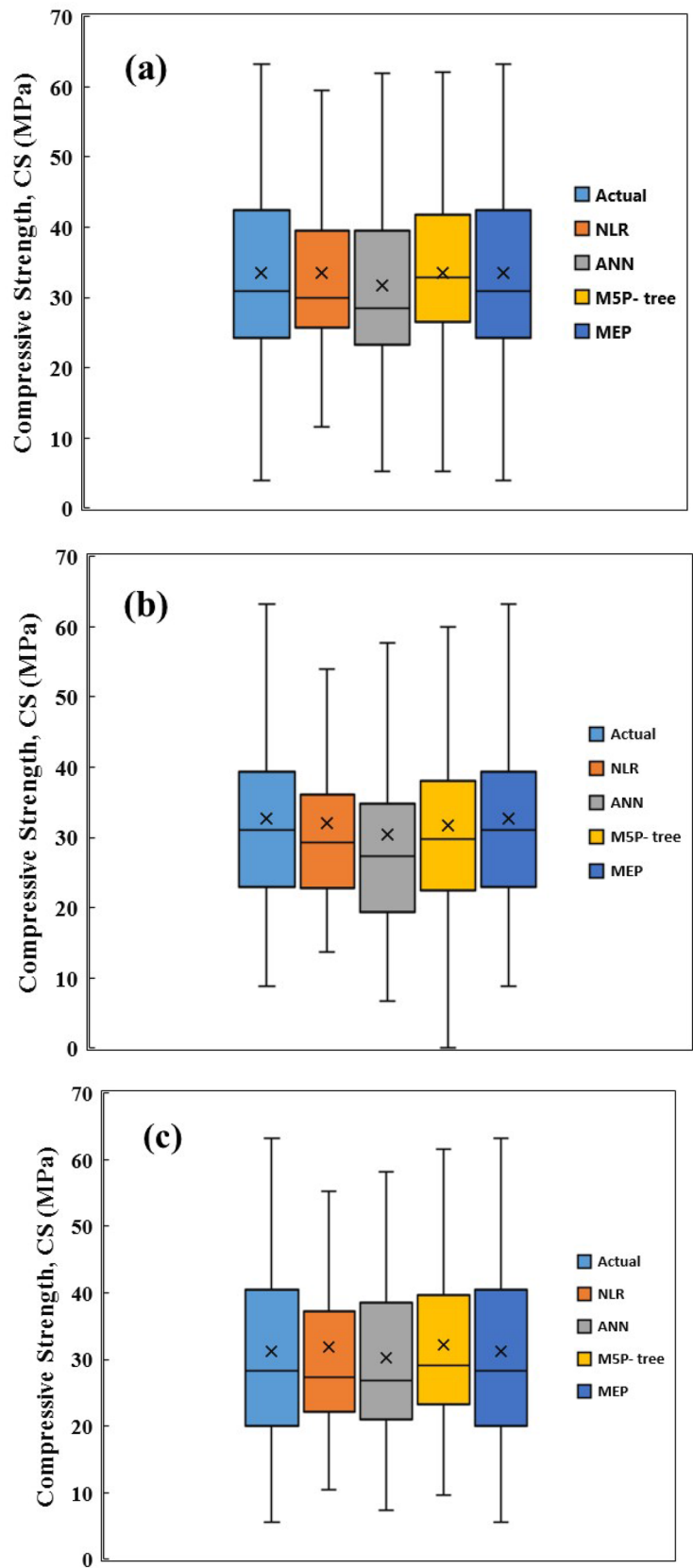
**Table 4** Summary of developed models performance

| Models | Fig.no. | Eq.no. | Training datasets | | | Testing datasets | | | Validating datasets | | |
|--------|---------|--------|-------------------|--|--|------------------|--|--|---------------------|--|--|
| | | | $R^2$ | RMSE (MPa) | MAE (MPa) | $R^2$ | RMSE (MPa) | MAE (MPa) | $R^2$ | RMSE (MPa) | MAE (MPa) |
| MEP | 6 | 17 | 0.87 | 4.86 | 3.23 | 0.88 | 3.88 | 2.77 | 0.897 | 4.72 | 3.35 |
| NLR | 7 | 18 | 0.84 | 5.39 | 3.83 | 0.85 | 4.28 | 3.35 | 0.81 | 6.35 | 4.95 |
| ANN | 10 | – | 0.9 | 4.23 | 2.89 | 0.86 | 4.15 | 3.03 | 0.88 | 5.07 | 3.76 |
| M5P-tree | 12 | 3 | 0.85 | 5.21 | 3.8 | 0.81 | 4.77 | 3.47 | 0.81 | 6.23 | 4.53 |

**Table 5** Sensitivity analysis for the model parameters using MEP model

| No | Combination | Removed parameter | RMSE (MPa) | MAE (MPa) | Ranking |
|----|-------------|-------------------|------------|-----------|---------|
| 1 | w/c, t, FA | – | 4.943 | 3.74 | – |
| 2 | t, FA | w/c | 10.75 | 7.35 | 2 |
| **3** | **w/c, FA** | **T** | **11.80** | **9.20** | **1** |
| 4 | w/c, t | FA | 5.35 | 4.10 | 3 |

**Data Availability** The data supporting the conclusions of this article are included with the article.

## Declarations

**Conflict of interest** The authors declare that they have no competing interests.

**Ethical Approval** Not applicable.

**Consent to Participate** Not applicable.

## References

1. Abed ZM (2018) The effect of using lightweight aggregate on some properties of cement mortar. Iraqi J Civ Eng 12(1):1–9
2. Gartner E (2004) Industrially interesting approaches to "low-CO2" cements. Cem Concr Res 34(9):1489–1498. https://doi.org/10.1016/j.cemconres.2004.01.021
3. Fraay ALA, Bijen JM, De Haan YM (1989) The reaction of fly ash in concrete a critical examination. Cem Concr Res 19(2):235–246. https://doi.org/10.1016/0008-8846(89)90088-4
4. Rahhal V, Talero R (2004) Influence of two different fly ashes on the hydration of portland cements. J Therm Anal Calorim 78(1):191–205. https://doi.org/10.1023/b:jtan.0000042167.46181.17
5. Peter C (2005) Hewlett, Lea's Chemistry of Cement and Concrete, vol 605. Wiley, New York, pp 10158–20012
6. Sakai E, Miyahara S, Ohsawa S, Lee S-H, Daimon M (2005) Hydration of fly ash cement. Cem Concr Res 35(6):1135–1140. https://doi.org/10.1016/j.cemconres.2004.09.008
7. Otsuka T, Mori S, Ishikawa M, Sakai E (2009) Relation between mineral compositions of fly ash and its pozzolanic reaction. Cem Sci Concr Technol 63(1):16–21
8. Bumrongjaroen W, Muller I, Schweitzer J, Livingston RA (2007) Application of glass corrosion tests to the reactivity of fly ash. World of Coal Ash, Northern Kentucky
9. Hassett DJ, Eylands KE (1997) Heat of hydration of fly ash as a predictive tool. Fuel 76(8):807–809. https://doi.org/10.1016/S0016-2361(97)00058-6
10. Kurda R, de Brito J, Silvestre JD (2017) Influence of recycled aggregates and high contents of fly ash on concrete fresh properties. Cement Concr Compos 84:198–213
11. Apostolopoulou M, Armaghani DJ, Bakolas A, Douvika MG, Moropoulou A, Asteris PG (2019) Compressive strength of natural hydraulic lime mortars using soft computing techniques. Proc Struct Integr 17:914–923. https://doi.org/10.1016/j.prostr.2019.08.122
12. Kurda R, Silvestre JD, de Brito J (2018) Life cycle assessment of concrete made with high volume of recycled concrete aggregates and fly ash. Resour Conserv Recycl 139:407–417
13. Kurda R, de Brito J, Silvestre JD (2017) Combined influence of recycled concrete aggregates and high contents of fly ash on concrete properties. Constr Build Mater 157:554–572
14. Kurda R, de Brito J, Silvestre JD (2019) Water absorption and electrical resistivity of concrete with recycled concrete aggregates and fly ash. Cem Concr Compos 95:169–182
15. Mahmood W, Mohammed A (2019) New Vipulanandan pq model for particle size distribution and groutability limits for sandy soils. J Test Eval 48(5):3695–3712. https://doi.org/10.1520/JTE20180606
16. Qadir W, Ghafor K, Mohammed A (2019) Evaluation the effect of lime on the plastic and hardened properties of cement mortar and quantified using Vipulanandan model. Open Eng 9(1):468–480. https://doi.org/10.1515/eng-2019-0055
17. Sihag P, Jain P, Kumar M (2018) Modelling of impact of water quality on recharging rate of storm water filter system using various kernel function based regression. Model Earth Syst Environ 4(1):61–68. https://doi.org/10.1007/s40808-017-0410-0
18. Marangu JMM (2020) Prediction of compressive strength of calcined clay based cement mortars using support vector machine and artificial neural network techniques. J Sustain Constr Mater Technol 5(1):392–398. https://doi.org/10.29187/jscmt.2020.43
19. Vipulanandan C, Mohammed A (2019) Magnetic field strength and temperature effects on the behavior of oil well cement slurry

modified with iron oxide nanoparticles and quantified with vipu-lanandan models. J Test Eval 48(6):4516–4537. https://doi.org/10.1520/JTE20180107

20. Mohammed A, Rafiq S, Sihag P, Kurda R, Mahmood W, Ghafor K, Sarwar W (2020) ANN, M5P-tree and nonlinear regression approaches with statistical evaluations to predict the compressive strength of cement-based mortar modified with fly ash. J Market Res 9(6):12416–12427. https://doi.org/10.1016/j.jmrt.2020.08.083

21. Alkayem NF, Shen L, Asteris PG, Sokol M, Xin Z, Cao M (2022) A new self-adaptive quasi-oppositional stochastic fractal search for the inverse problem of structural damage assessment. Alex Eng J 61(3):1922–1936

22. Armaghani DJ, Asteris PG (2021) A comparative study of ANN and ANFIS models for the prediction of cement-based mortar materials compressive strength. Neural Comput Appl 33(9):4501–4532

23. Asteris PG, Skentou AD, Bardhan A, Samui P, Lourenço PB (2021) Soft computing techniques for the prediction of concrete compressive strength using Non-Destructive tests. Constr Build Mater 303:124450

24. Asteris PG, Skentou AD, Bardhan A, Samui P, Pilakoutas K (2021) Predicting concrete compressive strength using hybrid ensembling of surrogate machine learning models. Cem Concr Res 145:106449

25. Asteris PG, Apostolopoulou M, Armaghani DJ, Cavaleri L, Chountalas AT, Guney D, Nguyen H (2020) On the metaheuristic models for the prediction of cement-metakaolin mortars compressive strength. Engineering 1:1(1).

26. Biricik H, Sarier N (2014) Comparative study of the characteristics of nano silica-, silica fume-and fly ash-incorporated cement mortars. Mater Res 17:570–582. https://doi.org/10.1590/S1516-14392014005000054

27. Burhan L, Ghafor K, Mohammed A (2020) Testing and evaluation of flowability, viscosity and long-term compressive strength of cement modified with polymeric admixture WR superplasticizer. IOP Publishing. https://doi.org/10.1088/1757-899X/737/1/012066

28. Xu A, Sarkar SL, Nilsson L-O (1993) Effect of fly ash on the microstructure of cement mortar. Mater Struct 26(7):414–424. https://doi.org/10.1007/BF02472942

29. Wong YL, Lam L, Poon CS, Zhou FP (1999) Properties of fly ash-modified cement mortar-aggregate interfaces. Cem Concr Res 29(12):1905–1913. https://doi.org/10.1016/S0008-8846(99)00189-1

30. Demir İ, Güzelkücük S, Sevim Ö (2018) Effects of sulfate on cement mortar with hybrid pozzolan substitution. Eng Sci Technol 21(3):275–283. https://doi.org/10.1016/j.jestch.2018.04.009

31. Jung S, Kwon S-J (2013) Engineering properties of cement mortar with pond ash in South Korea as construction materials: from waste to concrete. Open Eng 3(3):522–533. https://doi.org/10.2478/s13531-012-0068-3

32. Mishra S, Deodhar SV (2013) Effect of rice husk ash on cement mortar and concrete. New Build Mater Constr World 13:224–227

33. Türkel S, Altuntaş Y (2009) The effect of limestone powder, fly ash and silica fume on the properties of self-compacting repair mortars. Sadhana 34(2):331–343. https://doi.org/10.1007/s12046-009-0011-3

34. Puertas F, Amat T, Fernández-Jiménez A, Vázquez T (2003) Mechanical and durable behaviour of alkaline cement mortars reinforced with polypropylene fibres. Cem Concr Res 33(12):2031–2036. https://doi.org/10.1016/S0008-8846(03)00222-9

35. De Weerdt K, Haha MB, Le Saout G, Kjellsen KO, Justnes H, Lothenbach B (2011) Hydration mechanisms of ternary Portland cements containing limestone powder and fly ash. Cem Concr Res 41(3):279–291. https://doi.org/10.1016/j.cemconres.2010.11.014

36. Sasiekalaa K, Malathy R (2012) Behaviour of mortar containing silica fume and fly ash. J Ind Pollut Control 28:1–7

37. Alwash JJH (2013) Use of rice husk ash in cement mortar. Journal of University of Babylon 21(2):582–590

38. Tan Z, De Schutter G, Ye G, Gao Y (2013) The effect of limestone powder addition on strength of slag blended cement. Concrete under Severe Conditions: Environment and Loading (CONSEC-2013), vol 2, pp 1888–1898

39. Rai B, Kumar S, Satish K (2014) Effect of fly ash on mortar mixes with quarry dust as fine aggregate. Adv Mater Sci Eng. https://doi.org/10.1155/2014/626425

40. Holland JH (1992) Adaptation in natural and artificial systems: an introductory analysis with applications to biology, control, and artificial intelligence. MIT, New York

41. Asteris PG, Lourenço PB, Roussis PC, Adami CE, Armaghani DJ, Cavaleri L, Pilakoutas K (2022) Revealing the nature of metakaolin-based concrete materials using artificial intelligence techniques. Constr Build Mater 322, 126500

42. Parsajoo M, Mohammed AS, Yagiz S, Armaghani DJ, Khandelwal M (2021) An evolutionary adaptive neuro-fuzzy inference system for estimating field penetration index of tunnel boring machine in rock mass. J Rock Mech Geotech Eng 13(6):1290–1299

43. Parsajoo M, Armaghani DJ, Mohammed AS, Khari M, Jahandari S (2021) Tensile strength prediction of rock material using non-destructive tests: a comparative intelligent study. Transp Geotech 31, 100652.

44. Aho AV, Sethi R, Ullman JD (1986) Compilers, principles, techniques. Addison Wesley 7(8):9

45. Brameier M, Banzhaf W (2001) A comparison of linear genetic programming and neural networks in medical data mining. IEEE Trans Evol Comput 5(1):17–26. https://doi.org/10.1109/4235.910462

46. Handley S (1994, June) On the use of a directed acyclic graph to represent a population of computer programs. In: Proceedings of the first IEEE conference on evolutionary computation. IEEE World Congress on Computational Intelligence, pp 154–159. IEEE. https://doi.org/10.1109/ICEC.1994.350024

47. Mousavi SM, Gandomi AH, Alavi AH, Vesalimahmood M (2010) Modeling of compressive strength of HPC mixes using a combined algorithm of genetic programming and orthogonal least squares. Struct Eng Mech 36(2): p. 225–241. https://doi.org/10.12989/sem.2010.36.2.225

48. Emad, W., Salih, A., Kurda, R., Asteris, P. G., & Hassan, A. (2022). Nonlinear models to predict stress versus strain of early age strength of flowable ordinary Portland cement. European Journal of Environmental and Civil Engineering, 1–25.

49. Thongsanitgarn P, Wongkeo W, Sinthupinyo S, Chaipanich A (2012) Effect of limestone powders on compressive strength and setting time of Portland-limestone cement pastes. In: Advanced materials research, vol 343, pp 322–326. Trans Tech Publications Ltd. https://doi.org/10.4028/www.scientific.net/AMR.343-344.322

50. Quinlan JR (1992, November) Learning with continuous classes. In: 5th Australian joint conference on artificial intelligence, vol 92, pp 343–348. https://doi.org/10.1142/9789814536271

51. Faraj RH, Mohammed AA, Mohammed A, Omer KM, Ahmed HU (2021) Systematic multiscale models to predict the compressive strength of self-compacting concretes modified with nanosilica at different curing ages. Eng Comput 1:1–24

52. Mohammed AS (2017) Effect of temperature on the rheological properties with shear stress limit of iron oxide nanoparticle modified bentonite drilling muds. Egypt J Pet 26(3):791–802. https://doi.org/10.1016/j.ejpe.2016.10.018

53. Mohammed A, Mahmood W (2018) Statistical variations and new correlation models to predict the mechanical behavior and ultimate shear strength of gypsum rock. Open Eng 8(1):213–226. https://doi.org/10.1515/eng-2018-0026

54. Mohammed A, Mahmood W (2018) Vipulanandan failure models to predict the tensile strength, compressive modulus, fracture toughness and ultimate shear strength of calcium rocks. Int J Geotech Eng. https://doi.org/10.1080/19386362.2018.1468663

55. Ahmed HU, Mohammed AS, Mohammed AA, Faraj RH (2021) Systematic multiscale models to predict the compressive strength of fly ash-based geopolymer concrete at various mixture proportions and curing regimes. PLloS ONE 16(6):e0253006

56. Vipulanandan C, Mohammed AS (2014) Hyperbolic rheological model with shear stress limit for acrylamide polymer modified bentonite drilling muds. J Petrol Sci Eng 122:38–47. https://doi.org/10.1016/j.petrol.2014.08.004

57. Vipulanandan C, Mohammed A, Ganpatye AS (2018) Smart cement performance enhancement with NanoAl2O3 for real time monitoring applications using Vipulanandan models. OnePetro. https://doi.org/10.4043/28880-MS

58. Ojha RP, Verma CL, Denis DM (2018) Estimating unsaturated hydraulic conductivity function of sodic and normal soils using point source field dripper method. J Soil Water Conserv 17(1):34–40. https://doi.org/10.5958/2455-7145.2018.00005.X

59. Oladoye AO, Ige PO, Baurwa N, Onilude QA, Animashaun ZT (2020) Slenderness coefficient models for tree species in Omo biosphere reserve, South-western Nigeria. J Soc Trop Plant Res 7, 603

60. Kumar KM, Munjal ML (2018) Direct estimation and experimental validation of the acoustic source characteristics of two-cylinder naturally aspirated diesel engine exhaust system. Appl Acoust 135:70–84

61. Patel KB, Patel BR, Madhusudan MP (2009) Irrigation scheduling through water production function for rabi brinjal with surface and drip irrigation methods. In: Proceedings of the 13th international water technology conference, pp 557–561

62. Li M-F, Tang X-P, Wu W, Liu H-B (2013) General models for estimating daily global solar radiation for different solar radiation zones in mainland China. Energy Convers Manag 70:139–148. https://doi.org/10.1016/j.enconman.2013.03.004

63. Mohammed A., Rafiq S, Sihag P, Kurda R, Mahmood, W (2020) Soft computing techniques: systematic multiscale models to predict the compressive strength of HVFA concrete based on mix proportions and curing times. J Build Eng. https://doi.org/10.1016/j.jobe.2020.101851.